

# Common energy scale for magnetism and superconductivity in cuprates

Amit Keren and Amit Kanigel

*Physics Department, Technion-Israel Institute of Technology, Haifa 32000, Israel*

(Received 23 September 2002; revised manuscript received 13 February 2003; published 28 July 2003)

Many compounds based on  $\text{CuO}_2$  planes (cuprates) superconduct below a critical temperature  $T_c$ . Some of them show a second phase where a spontaneous static magnetic field appears below a critical temperature  $T_g$ , which is lower than  $T_c$ . By comparing  $T_c$  and  $T_g$  in numerous superconducting families, each with its own maximum  $T_c$ , we find that the same energy scale determines both critical temperatures. This clearly indicates that the origin of superconductivity in the cuprates is magnetic.

DOI: 10.1103/PhysRevB.68.012507

PACS number(s): 74.25.Ha, 74.25.Dw, 76.75.+i

One of the most challenging tasks of solid-state physics today is to understand the mechanism for superconductivity in cuprates. These materials, which have a relatively high critical temperature  $T_c$ , are based on doped  $\text{CuO}_2$  planes. Since at zero doping they are antiferromagnets, several theories ascribe their superconductivity to holes interacting via a magnetic medium.<sup>1,2</sup> Yet the phenomenon of superconductivity begins at doping levels in which magnetism almost disappears, and therefore there is no clear evidence relating the two. Fortunately, there is a narrow doping range in which superconductivity and magnetism, in the form of randomly oriented static spins (a spin glass), coexist below a critical temperature  $T_g < T_c$ . We thus focus on this doping range and examine  $T_g$  and  $T_c$  in numerous superconducting families, which are distinct in the sense that each one has its own maximum  $T_c$  [ $T_c^{\text{max}}$ ]. We find that in all cases a common energy scale controls both critical temperatures. Therefore, magnetism and superconductivity in the cuprates are different facets of the same Hamiltonian.

The families for which both  $T_g$  and  $T_c$  data exist are  $(\text{Ca}_x\text{La}_{1-x})(\text{Ba}_{1.75-x}\text{La}_{0.25+x})\text{Cu}_3\text{O}_{6+y}$  (CLBLCO),<sup>3</sup>  $\text{La}_{2-y}\text{Sr}_y\text{CuO}_4$  (LSCO),<sup>4,5</sup>  $\text{Y}_{1-y}\text{Ca}_y\text{Ba}_2\text{Cu}_3\text{O}_6$  (YCBCO),<sup>4</sup>  $\text{Bi}_{2.1}\text{Sr}_{1.9}\text{Ca}_{1-x}\text{Y}_x\text{Cu}_2\text{O}_{8+y}$  (Bi-2212),<sup>5</sup> and  $\text{YBa}_2\text{Cu}_3\text{O}_{6+y}$  (YBCO).<sup>6</sup> Several groups including ours gathered the data, and the determination of  $T_g$  was done using the  $\mu\text{SR}$  technique. In this technique one implants fully polarized positive muons in a sample and measures the time dependence of their polarization  $P_z(t)$ . This polarization changes dramatically when static magnetic fields appear. This is demonstrated for a superconducting compound from the CLBLCO family with  $T_c = 33.1$  K in Fig. 1, which is taken from Ref. 3 for completion. Between  $T = 40$  and 8 K,  $P_z(t)$  is typical for muon polarization in an environment where the magnetic field emanates from nuclear moments. We denote this polarization by  $P_z^\infty(t)$ . At about  $T = 7.4$  K a fast relaxation component appears, which is due to some additional strong magnetic field. As the temperature is lowered the fast relaxing component grows at the expense of the slow one, and at a temperature of 0.37 K, no slow relaxing component is observed. In addition, at this temperature the polarization saturates at long times at one-third of its initial value. This is typical for randomly frozen magnetic fields where one-third of the fields happen to point in the direction of the muon spin.

In order to determine  $T_g$  quantitatively all authors effectively fit their data to

$$P_z(t) = A_m \exp[-(\lambda t)^\beta] + A_n P_z^\infty(t), \quad (1)$$

where  $\lambda$  is a relaxation rate, and the amplitudes  $A_m$  and  $A_n$  represent muons in magnetic and normal environments. However, different authors use different parameters in the fit function for the determination of  $T_g$ . We will show below that this has no bearing on our final conclusion. In particular, we fit Eq. (1) to the data in Fig. 1 with  $\beta = 1/2$  and  $A_m + A_n$  common to all temperatures. In Fig. 2 we present  $A_m$  as a function of temperature for three different samples of the CLBLCO family with  $x = 0.3$ . As expected  $A_m$  grows as the temperature decreases and saturates. Our criterion for  $T_g$  is the temperature at which  $A_m$  is half of its saturation value as demonstrated by the vertical lines. This figure demonstrates the sensitivity of  $T_g$  to doping.

In order to quantify the relation between  $T_g$  and  $T_c$ , we distinguish between two kinds of holes. The first kind we call *mobile holes*, and their doping level is  $p_m$ . The second kind is the usual *chemical holes*, and their doping level is denoted by  $p$ . The reason for this distinction is that the only experimental known value is that of the chemical formula of the compounds, namely, the  $x$  and  $y$  values. Theoretical arguments relate  $x$  and  $y$  to  $p$ ,<sup>7-9</sup> but the accuracy of these relations is debatable.<sup>9</sup> By introducing  $p_m$  we allow for an additional scaling parameter, which could be determined

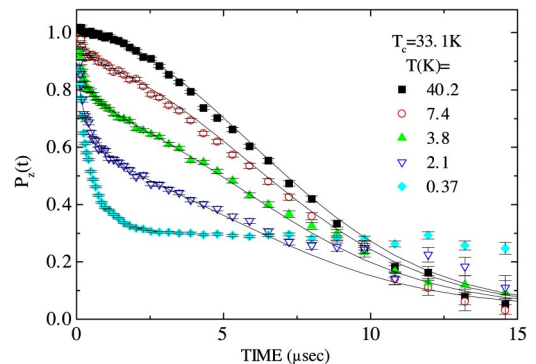


FIG. 1. (Color online)  $\mu\text{SR}$  spectra obtained in a  $x = 0.1$ ,  $y = 7.012$  CLBLCO sample at various temperatures. The solid lines are fits using Eq. (1). Taken from Ref. 3.

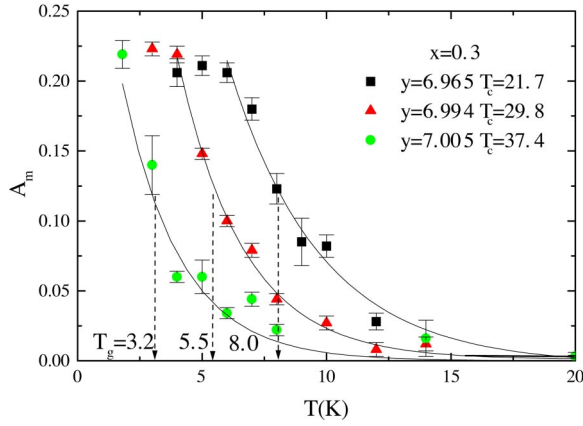


FIG. 2. (Color online) The magnetic amplitude  $A_m$  as a function of temperature for different  $(\text{Ca}_x\text{La}_{1-x})(\text{Ba}_{1.75-x}\text{La}_{0.25+x})\text{Cu}_3\text{O}_y$  samples. The solid lines are guides to the eye.  $T_g$  is the temperature at which  $A_m$  is half of its saturation value, as demonstrated by the dashed lines. Taken from Ref. 3.

experimentally, and could lead to a comparison between different compounds. An equally good name for  $p_m$  could have been “corrected hole doping.” The scaling parameter is determined as follows. First, we convert the  $T_g$  and  $T_c$  values of all material to be functions of  $p$ . The case of LSCO, YBCO, and Bi-2212 is immediate since the authors of Refs. 4 and 5 present their data in this way. For CLBLCO, however,  $T_g$  and  $T_c$  are given as a function of  $y$ .<sup>3</sup> We assume the relation  $p = -0.205 + y/3$  obtained from simple valance counting. In the case of YBCO, the  $y$  to  $p$  conversion is taken from Presland *et al.*<sup>10</sup> Second, we define  $p^{opt}$  as chemical hole doping at optimum, where optimum means  $T_c^{max}$ , and introduce  $\Delta p = p - p^{opt}$ . Finally, we write

$$\Delta p_m = K_f \Delta p, \quad (2)$$

where  $K_f$  is the scaling parameter that is different for the various cuprate families. We interpret  $\Delta p_m$  as  $p_m - p_m^{opt}$  where  $p_m^{opt}$  is the number of mobile holes at optimum. This point requires extra attention; the scaling we perform between chemical and mobile holes is done by counting them from optimum, and not from  $p=0$ . We determine  $K_f$  from experimental data by making  $T_c/T_c^{max}$ , for all the families, collapse onto one curve, resembling the curve of  $\text{La}_{2-y}\text{Sr}_y\text{CuO}_4$ , since in this case it is believed that  $p_m = p$ . This is demonstrated in Fig. 3(a). It should be pointed out that LSCO serves only as a reference, and whether  $p_m = p$  for this compound or not has no bearing on our conclusions. A summary of  $p^{opt}$ ,  $K_f$ , and  $T_c^{max}$  is given in Table I. In Fig. 3(b) we also plot  $T_g/T_c^{max}$  as a function of  $\Delta p_m$  (using the previously determined values of  $K_f$ ). Magically,  $T_g/T_c^{max}$  also collapse onto one line for all the cuprates we have examined. The line, depicted in Fig. 3(b), is described by

$$T_g/T_c^{max} = -2.5\Delta p_m - 0.15. \quad (3)$$

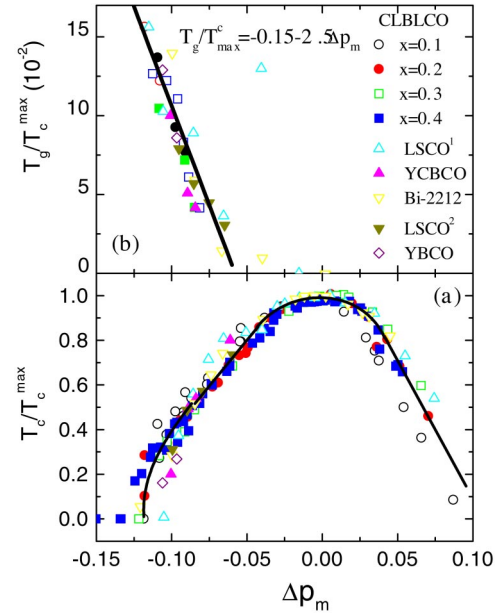


FIG. 3. (Color online) (a)  $T_c/T_c^{max}$  and (b)  $T_g/T_c^{max}$  as a function of  $\Delta p_m = K_f \Delta p$  [see Eq. (2)].  $K_f$  is chosen so that  $T_c/T_c^{max}$  vs  $\Delta p_m$  domes of various cuprate families collapse into a single curve. As a consequence  $T_g/T_c^{max}$  vs  $\Delta p_m$  also collapses into a single line.

Up to date this type of scaling was demonstrated only for the CLBLCO family.<sup>3</sup>

It is important to mention that Eq. (3) is independent of the criteria used to determine  $T_g$ . In the case of LSCO, for example,  $T_g$  was determined from Eq. (1) by two different methods. (1) the temperature at which  $\beta = 1/2$ , a behavior typical of spin glasses at  $T_g$ .<sup>5</sup> (2) the temperature where  $\lambda$ , obtained only from fit to the long time data with  $\beta = 1$ , has a peak—a common feature of all magnets upon freezing.<sup>4</sup> Both methods agree with each other.<sup>5</sup>

We interpret the scaling of Fig. 3 as follows. The Uemura relations<sup>12</sup> and recent theories of hole pair boson motion in

TABLE I. Showing the optimal chemical doping, the scaling factor used in Eq. (2) to produce  $\Delta p_m$ , and the maximum  $T_c$  for the various compounds presented in Fig. 3. The  $T_c^{max}$  (and  $p^{opt}$ ) of YBCO is not known, and the values given in the table are assumed. Only two samples of YBCO, for which both  $T_g$  and  $T_c$  have been measured, are shown.

HTSC Family	$P_{opt}$	$K_f$	$T_c^{max}$
CLBLCO $x=0.1$	0.18	2.0	58
CLBLCO $x=0.2$	0.18	1.9	69
CLBLCO $x=0.3$	0.18	1.8	77
CLBLCO $x=0.4$	0.18	1.5	80
LSCO	0.16	1.0	38
YBCO	0.16	1.1	65
Bi-2212	0.16	1.1	44
YBCO	0.16	1.0	93
LSCO $x=0.01$	0.16	1.5	26
LSCO $x=0.01$	0.18	2	17

an antiferromagnetic background<sup>2</sup> suggest that  $T_c$  is proportional to  $n_s$  with a proportionality constant  $J_f$ , where the subscript  $f$  stands for family, namely,

$$T_c = J_f n_s(\Delta p_m). \quad (4)$$

The reason different families have different  $T_c^{\max} = J_f n_s(0)$  is because  $J_f$  varies from one family to the next, but  $n_s(\Delta p_m)$  does not. Therefore,

$$T_c / T_c^{\max} = n_s(\Delta p_m) / n_s(0) \quad (5)$$

is a function of  $\Delta p_m$  for all cuprate families. Using Eq. (3) this gives

$$T_g = J_f n_s(0) (-2.5\Delta p_m - 0.15).$$

Thus, the successes of the simultaneous scaling of  $T_c$  and  $T_g$  for all the compounds discussed here suggests that the same energy scale  $J_f$  controls both the superconducting and magnetic transitions in all cuprates.

At first this result seems surprising, since it is believed that in the antiferromagnetic phase of the cuprates, there are three magnetic energy scales. The isotropic in-plane Heisenberg coupling  $J$ , and the in-plane and out-of-plane anisotropy energies  $J\alpha_{xy}$  and  $J\alpha_{\perp}$ , respectively. However, Keimer *et al.* showed that the Néel temperature  $T_N$  depends only logarithmically on both anisotropies  $\alpha_{xy}$  and  $\alpha_{\perp}$ .<sup>11</sup> It is conceivable that this is also the situation in the glassy phase. In that case the energy scale of  $T_g$  will be set only by  $J$ . Another two-dimensional theory that appears to support the existence of glassy freezing is given in Ref. 13.

Further insight could be achieved by assuming a linear relation between  $n_s$  and  $\Delta p_m$ , namely,

$$n_s(\Delta p_m) = \alpha(p_m^{\text{opt}} + \Delta p_m). \quad (6)$$

If all the mobile holes had turned into the Cooper pairs we would have  $\alpha = 1/2$ . Taking  $p_m^{\text{opt}} = 0.16$ , we find from Eqs. (3) and (6)

$$T_g / T_c^{\max} = 0.3[1 - c_g \times n_s(\Delta p_m)], \quad (7)$$

where  $c_g = 8/\alpha$ . This equation could be used to predict  $T_g$  for compounds in which the magnetic transition is not found yet.

Finally, it is important to demonstrate that the simultaneous scaling of  $T_g$  and  $T_c$  is a property of clean superconductors and does not work in all cases. A perfect example for a scaling failure is given by  $\text{La}_{2-y}\text{Sr}_y\text{Cu}_{1-x}\text{Zn}_x\text{O}_4$ .<sup>5</sup> Here samples with the same amount of Zn are considered to be

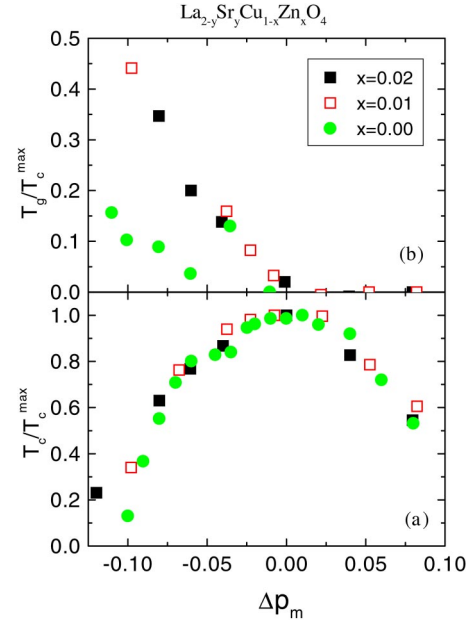


FIG. 4. (Color online) (a)  $T_c / T_c^{\max}$  and (b)  $T_g / T_c^{\max}$  as a function of  $\Delta p_m = K_f \Delta p$  [see Eq. (2)].  $K_f$  is chosen so that  $T_c / T_c^{\max}$  vs  $\Delta p_m$  domes for various  $\text{La}_{2-y}\text{Sr}_y\text{Cu}_{1-x}\text{Zn}_x\text{O}_4$  compounds, representing impure cases, collapse into a single curve. The same scaling does not apply to  $T_g$ .

one family of HTSC with its own  $T_c^{\max}$ . The reduction of  $T_c^{\max}$  with increasing Zn concentration is a result of the increasing impurity scattering rates, since the Zn reside in the  $\text{CuO}_2$  plane. As demonstrated in Fig. 4, the scaling transformation that makes all  $T_c$  vs  $\Delta p_m$  domes collapse into one function does not apply for  $T_g$  vs  $\Delta p_m$ . The parameters used to generate this plot are also given in Table I. The failure of the scaling suggests that a mechanism with a different energy scale is involved in the reduction of  $T_c$  when impurities are present. Interestingly, the two data sets of  $T_g / T_c^{\max}$  vs  $\Delta p_m$  for the impure cases do fall on the same line.

We conclude that the variation of  $T_c$  between different superconducting families, based on  $\text{CuO}_2$  planes, is a consequence of variations in the strength of the magnetic interactions.

We would like to thank the PSI and ISIS facilities for their kind hospitality and continuing support of this project. We acknowledge very helpful discussions with A. Auerbach and E. Altman. We are grateful to S. Sanna and R. Derenzi for providing their data prior to publication. The Israeli Science Foundation and the EU-TMR program funded this work.

<sup>1</sup>Amnon Aharony, R.J. Birgeneau, A. Coniglio, M.A. Kastner, and H.E. Stanley, Phys. Rev. Lett. **60**, 1330 (1988); P. Monthoux, A.V. Balatsky, and D. Pines, *ibid.* **67**, 3448 (1991).

<sup>2</sup>V.J. Emery and S.A. Kivelson, Nature (London) **374**, 434 (1995); S.-C. Zhang, J.-P. Hu, E. Arrigoni, W. Hanke, and A. Auerbach, Phys. Rev. B **60**, 13 070 (1999); E. Altman and A. Auerbach,

Phys. Rev. B **65**, 104508 (2002).

<sup>3</sup>A. Kanigel, A. Keren, Y. Eckstein, A. Knizhnik, J.S. Lord, and A. Amato, Phys. Rev. Lett. **88**, 137003 (2002).

<sup>4</sup>Ch. Niedermayer, C. Bernhard, T. Blasius, A. Golnik, A. Moodenbaugh, and J.I. Budnick, Phys. Rev. Lett. **80**, 3843 (1998).

<sup>5</sup>C. Panagopoulos, J.L. Tallon, B.D. Rainford, T. Xiang, J.R. Co-

- per, and C.A. Scott, Phys. Rev. B **66**, 064501 (2002).
- <sup>6</sup>S. Sanna, G. Allodi, and R. De Renzi, Solid State Commun. **126**, 85 (2003).
- <sup>7</sup>I.D. Brown, J. Solid State Chem. **81**, 122 (1989); **90**, 155 (1991).
- <sup>8</sup>J.L. Tallon, Physica C **168**, 85 (1990).
- <sup>9</sup>O. Chmaissem, Y. Eckstein, and C.G. Kuper, Phys. Rev. B **63**, 174510 (2001).
- <sup>10</sup>M.R. Preslan *et al.*, Physica C **176**, 95 (1991).
- <sup>11</sup>B. Keimer *et al.*, Phys. Rev. B **45**, 7430 (1992)
- <sup>12</sup>Y.J. Uemura *et al.*, Phys. Rev. Lett. **62**, 2317 (1989).
- <sup>13</sup>T. Pereg-Barnea and M. Franz, Phys. Rev. B **67**, 060503(R) (2003).